The dynamics of water in protein solutions: The field dispersion of deuterium NMR longitudinal relaxation

Abstract

The analysis of the field dispersion of the ^{2}H-NMR longitudinal relaxation of water in lysozyme, bovine serum albumin (BSA), alkaline phosphatase and hemocyanin solutions was attempted. In all cases, two independent relaxation contributions are required in order to fit the data. For typical globular proteins, the shortest correlation time (10^{-8} s) is identified with the rotational correlation time of the protein monomer. A second correlation time (10^{-7} s) is attributed to protein polydispersity.

Keywords: Protein hydration; Water dynamics; Deuterium NMR field dispersion.

1. Introduction

Nuclear Magnetic Resonance (NMR) relaxation is a major technique for the assessment of the dynamic state of water and the extent of its perturbation in solutions and heterogeneous systems [1–6]. However, despite the related intensive research, most of the previously identified outstanding problems in the field [7] are still subjects of debate.

NMR studies of protein hydration have mostly involved relaxation measurements of the ^{1}H, ^{2}H, and ^{17}O nuclei of the water molecule, in this order of decreasing frequency of application. The analysis of ^{1}H-NMR data is complicated by cross-relaxation between water and protein protons [8,9] as well as proton chemical exchange [36]. There is evidence that deuterium chemical exchange between ^2H_2O and protein ionizable groups may significantly contribute to the ^{2}H-NMR relaxation of water [10,11] and needs to be taken into account. Oxygen-17, being unaffected by such complications, is the nucleus of choice for the study of protein hydration [12].

The usual approach to the study of protein hydration of NMR is the measurement of NMR relaxation times as a function of temperature [2–5], protein concentration [4,6] and magnetic

field strength [13–15]. The latter type of experiment requires specialized field-cycling instrumentation ([14,15] and references therein) that is not widely available; with such equipment one can readily measure proton or deuterium T_1's (but not T_2's) as a function of magnetic field strength. The fast NMR relaxation of oxygen-17 nuclei precludes similar ^{17}O-NMR measurement. As a result, there are limited ^{17}O-NMR field dispersion data that have been obtained by conventional, single-field NMR spectrometers which describe only part of the frequency dependence [12].

The general observation in NMR frequency dependence experiments is that, in the presence of a protein, the longitudinal NMR relaxation rate $R_1 = 1/T_1$ of water nuclei is field-independent at very low NMR frequencies; it gradually decreases with increasing magnetic field strength/NMR frequency and finally it becomes field-independent. Its high-frequency value is higher than the frequency-independent relaxation rate of pure water and the inflection point of the dispersion is related to the protein rotational correlation time [12–14]. Field dispersion data are valuable because they fully describe the spectral density function(s) that characterize the various dynamic processes in the system which are responsible for NMR relaxation. In the case of a globular protein in solution, water molecules are generally thought to exchange between a 'free' (bulk water) and a 'bound' (hydration water) state with an approximate lifetime of 10^{-5}–10^{-6} s [2]; 'bound' water molecules also reorient with the protein (correlation time of the order of 10^{-8}–10^{-9} s) and diffuse along the protein surface on a timescale of 10^{-7} s [2,37]. Other possible dynamic processes that involve 'bound' water molecules include the motion (10^{-10}–10^{11} s) of hydrated protein side chains [49,50], the fast rotation (10^{-11} s) of water molecules around their bonding axis to the protein surface [7] and the chemical exchange (10^{-4} s) of hydrogen between water molecules and protein ionizable groups as well as that between 'bound' and 'free' water molecules [2,36]. These timescales should be compared to the translation/rotation of 'free' water molecules (10^{-12} s) and the proton exchange between 'free' water molecules with a lifetime of the order of 10^{-4} s [2,36]. The contribution to the NMR relaxation due to motions faster than 10^{-10} s is frequency-independent in the experimentally accessible NMR frequency range.

Previous estimates of protein rotational correlation times from field dispersion data have yielded conflicting and unrealistically high values [10–15,39]. It is the purpose of the present study to re-evaluate the available ^{2}H-NMR field dispersion data in an attempt to reconcile the analysis results with the known protein physico-chemical properties.

2. Theory

The simplest possible model of protein hydration is a two-state one where water exchanges chemically between a dilute B ('bound') and an abundant F ('free') state; the observed longitudinal relaxation time will then be [38]:

$$\frac{1}{T_{1,\mathrm{obs}}} = \frac{P_\mathrm{B}}{T_{1\mathrm{B}} + \tau_\mathrm{m}} + \frac{P_\mathrm{F}}{T_{1\mathrm{F}}} \qquad (1)$$

where P_B and P_F are the 'bound' and 'free' fractions of total water ($P_\mathrm{B} + P_\mathrm{F} = 1$; $P_\mathrm{B} \ll P_\mathrm{F} \sim 1$) and τ_m is the lifetime of a water molecule in the 'bound' state. An underlying assumption in the derivation of eq. (1) is that $T_{1\mathrm{B}} \ll T_{1\mathrm{F}}$, a condition readily fulfilled in the case of ^{2}H-NMR of typical globular proteins where $T_{1\mathrm{B}} \sim 10^{-4}$ s and $T_{1\mathrm{F}} \sim 10^{-1}$ s. Since $T_{1\mathrm{B}} \sim 10^{-4}$ s $\gg \tau_\mathrm{m} \sim 10^{-6}$ s (fast exchange condition), eq. (1) is simplified to

$$R_{1,\mathrm{obs}}(\omega) = P_\mathrm{B} R_{1\mathrm{B}}(\omega) + P_\mathrm{F} P_{1\mathrm{F}} \qquad (2)$$

where the relaxation times have been replaced by the corresponding relaxation rates ($R_1 = 1/T_1$) and the frequency-dependent relaxation rates $R_{1,\mathrm{obs}}$ and $R_{1\mathrm{B}}$ are distinguished from the frequency independent $R_{1\mathrm{F}}$. According to the general theory of quadrupolar relaxation through molecular reorientation [16]:

$$R_{1\mathrm{B}}(\omega) = \alpha + \beta\left(\frac{0.2}{1+\omega^2\tau_\mathrm{c}^2} + \frac{0.8}{1+4\omega^2\tau_\mathrm{c}^2}\right). \qquad (3)$$

In eq. (3), all possible frequency-independent contributions to R_{1B} are lumped together in α.

If the motion of 'bound' water is *isotropic*, then

$$\beta = \frac{3\pi^2}{10}\frac{2I+3}{I^2(2I-1)}K^2\left(1+\frac{\eta^2}{3}\right)\tau_c \qquad (4)$$

Alternatively, if water molecules 'bound' to the protein can rotate anisotropically with a slow (ns) and a fast (ps) motion [7,10–12,46], then

$$\beta = \frac{3\pi^2}{10}\frac{2I+3}{I^2(2I-1)}K^2S^2\tau_{Bs} \qquad (5)$$

where $\omega = 2\pi\nu$ is the angular precession frequency, ν being the NMR frequency used, $\tau_c = \tau_{Bs}$ is the correlation time associated with the nanosecond motion of 'bound' water, I is the nuclear spin quantum number, $K = e^2qQ/h$ is the nuclear quadrupole coupling constant, η is the asymmetry parameter for the electric field gradient at the nucleus, and S is the order parameter that describes the orientation of water near the protein surface. In the case of ^{2}H-NMR relaxation measurements, $I = 1$, $K = 216.4$ kHz and $\eta = 0.1$ [17]. For isotropic binding $S = 1$; in the anisotropic case, estimates of S range from 0.12 to 0.23 [6].

Three independent dynamic processes need to be considered for the 'bound' water molecules: radial diffusion perpendicular to the protein surface (i.e., 'bound'–'free' chemical exchange), lateral diffusion parallel to the protein surface, and the rotation of the protein itself [18]; they are characterized, respectively, by the correlation times τ_{rad}, τ_{lat}, and τ_{rot}. Then

$$\frac{1}{\tau_{Bs}} = \frac{1}{\tau_{rad}} + \frac{1}{\tau_{lat}} + \frac{1}{\tau_{rot}} \qquad (6)$$

A consequence of eq. (6) is that, as intuitively expected, the fastest of the dynamic processes mentioned above dominates the observed field dispersion. Since for a moderately sized globular protein $\tau_{rot} \sim 10^{-8}$ s $< \tau_{lat} \sim 10^{-7}$ s $< \tau_{rad} \sim 10^{-6}$ s (τ_{rad} being essentially the lifetime of a water molecule in the 'bound' state) it follows that $\tau_{Bs} \sim \tau_{rot}$; indeed, data show an increase of τ_{Bs} with protein size [14].

In the case of more than one relaxation contributions

$$R_{1,obs} = \sum_i R_1(\omega, \tau_{ci}) \qquad (7)$$

where

$$R_1(\omega, \tau_{ci}) = A + B\left(\frac{0.2\tau_{ci}}{1+\omega^2\tau_{ci}^2} + \frac{0.8\tau_{ci}}{1+4\omega^2\tau_{ci}^2}\right) \qquad (8)$$

This may be the case for coexisting protein species (e.g., monomer and oligomer) where distinct populations of 'bound' water need to be considered. The high protein concentrations that are being used for NMR relaxation measurements of protein hydration (typically 10–20%) can lead to protein aggregation due to protein-protein interactions [6,11] even under experimental conditions that favor monomer formation.

3. Methods

3.1 Relaxation data

In the present study we have made use of the deuterium field dispersion data for hen egg-white lysozyme, *Helix pomatia* α-hemocyanin, and *E. coli* alkaline phosphatase reported by Koenig and coworkers [9,13,14] and those for bovine serum albumin (BSA) at various protein concentrations reported by Schauer et al. [15]. Data were obtained from enlarged field dispersion figures from the original reports, using a coordinate digitizer interfaced to a Modcomp classic minicomputer to maintain a high degree of precision.

Lysozyme undergoes reversible association–dissociation in the pH range from 5 to 9 that depends on ionic strength, temperature, and protein concentration ([22–24] and references therein). At pH 4.6 and 22°C, lysozyme is predominantly in the monomeric form; high protein concentrations (e.g., 210 mg/ml), low temperatures (e.g., 4°C) and the absence of salt are expected for favor protein aggregation [22,23,11].

In order to extend the field dispersion data sets for lysozyme reported by Koenig et al. [13] to higher NMR frequencies, additional deuterium-T_1 measurements by inversion recovery were carried out at 22 ± 1°C and 5 ± 2°C using a Bruker MSL300 (46.07 MHz) and a JEOL GX400 (61.37 MHz) spectrometer. Lysozyme (Sigma, St. Louis, MO) was dissolved in 80% ^2H_2O–20% ^1H_2O to a spectrophotometrically determined ($E^{1\%}_{1\,cm} = 26.0$ at 280 nm) concentration of 214 mg/ml; its pH was adjusted to 4.55 with 2*N* HCl (uncorrected pH meter reading). The measured solvent relaxation rates at 22°C (2.5 s^{-1}) and 5°C (4.7 s^{-1}) were identical to those in the original report [14].

E. coli alkaline phosphatase in 0.25 *M* Tris solutions at pH/pD 7.5–8.0 and 5°C is predominantly a dimer with a molecular weight of 85,000 [26,27].

The pH/pD of the bovine serum albumin solutions in ^2H_2O was not provided in the original report [15], thus not allowing an estimate of the protein's conformation/state of aggregation. In the absence of any pH/pD adjustment, the sample's pD should be around 6. The molecular weight (MW) of monomeric BSA is 66,000 a.m.u. but it is known that lyophilized BSA preparations also contain considerable amounts of dimers and higher polymers [28].

The experimental conditions during the α-hemocyanin measurements (Fig. 2) favor the undissociated (MW ~ 9 10^6) protein [30,32]. The combined effect of temperature (25°C) and pH/pD (ca. 7.5 if corrected for the isotopic composition of water) may result in approximately 10% dissociation to half molecules [30,31].

Information about the size and shape of the proteins used in the present study is summarized in Table 1.

3.2 Data analysis

We have modelled the field dispersion data with eq. (8), i.e.

$$R_1 = A + Bf(\omega, \tau_c) \tag{9}$$

where

$$f(\omega, \tau_c) = \frac{0.2\tau_c}{1+\omega^2\tau_c^2} + \frac{0.8\tau_c}{1+4\omega^2\tau_c^2} \tag{10}$$

and also with an extension of it,

$$R_1 = A + B_1 f(\omega, \tau_{c1}) + B_2 f(\omega, \tau_{c2}) \tag{11}$$

and for certain samples that showed a distinct low-field dispersion (i.e., 25% or 33% w/w BSA —see Fig. 4) that are presumably due to pronounced protein aggregation the expression

$$R_1 = A + B_1 f(\omega, \tau_{c1}) + B_2 f(\omega, \tau_{c2}) + B_3 f(\omega, \tau_{c3}) \tag{12}$$

Nonlinear regression analysis of all field dispersion data was performed using the RS/1 software package (BBN Software Products, Cambridge, MA). Calculations were carried out on a VAX 8350 computer. For the various comparison of the goodness of fit, the *F*-test was used [34] with the following *F*-value:

$$F = \frac{(SSR_1 - SSR_2)/(df_1 - df_2)}{SSR_2/df_2} \tag{13}$$

Table 1

The size and shape for the proteins at the employed experimental conditions

Protein	Aggregation state (MW, Da)	Shape and Size [Ref.]
Lysozyme	Mostly monomer (14,300)	Prolate ellipsoid 45×30×30 Å [a] [13,25]
Alkaline phosphatase	Mostly dimer (85,000)	Compact sphere, 60 Å diameter [a] [14,26,33]
BSA	Monomer (66,000) plus aggregates of unknown size	Prolate ellipsoid (monomer), 141×41×41 Å [b] [15,28]
Hemocyanin	90% undissociated (9 10^6)	Hollow cylinder, height×diam. = 380×300 Å [a] [13,29,31]

[a] Excluding water of hydration; a 3-Å thick 'bound' water layer must be also taken into consideration.
[b] Hydrated.

where *SSR* refers to the sum of square of the residuals and *df* to the number of the degrees of freedom (number of data points minus of fitting parameters). The subscript '1' refers to the simpler model, the one with the fewer parameters. *F*-distribution tables [35] were consulted for ($df_1 - df_2$) and df_2 degrees of freedom at the 10% and 5% levels of statistical significance (typical error in T_1 measurements).

4. Results and discussion

4.1 Evaluation of the results

The results of the field dispersion data analysis according to eqs. (9)–(12) are provided in Tables 2–4; fittings are shown in Figs. 1–4. The *F*-test showed that more than a single dispersion is required in all cases (1% level or below). Lysozyme, phosphatase, 10% BSA, and hemocyanin data require five-parameter fittings (Table 3) whereas seven-parameter fittings are required for 25% and 33% BSA (Table 4).

The large errors in τ_c for some data sets (i.e., lysozyme at 22°C and 25% or 33% BSA) are most likely due to the small number of data points (Fig. 1A) and/or their significant scattering in the particular frequency range (BSA). This may also be the reason for the apparent discrepancy in τ_c values for lysozyme in Table 3 where τ_c decreases with decreasing temperature; additional measurements at the high-frequency end of the dispersion are required for an unambiguous determination of τ_c's for lysozyme at 22°C.

The 10% BSA data may actually require three dispersions but the considerable noise at low frequencies does not allow a six- or seven-parameter fitting. The effects of polydispersity are most pronounced for the 33% BSA sample which requires a seven-parameter fitting (Table 4). The results for the 25% BSA sample are out of line from those obtained for 10% and 33% BSA (Tables 3 and 4). Extensive aggregation during sample handling (evident as a pronounced low frequency dispersion that is absent from the other BSA data sets) may be the reason; the 25% BSA results were not considered during the data analysis.

4.2 Correlation times

Estimates of τ_{rot} for the various proteins (Table 5) are in good agreement with the shortest correlation times τ_{c1} that we obtained: 18.7 ns for lysozyme at 4°C (Table 3), 82.7 ns for alkaline. phosphatase (Table 3) and 40.3–47.4 ns for BSA (Tables 3 and 4); hemocyanin (Table 3) is a notable exception as discussed below. For typical globular proteins, the shortest correlation time τ_{c1} obtained from the field dispersion of ^{2}H-NMR longitudinal relaxation can be identified with the correlation time for isotropic protein rotation, τ_{rot}. It should be noted that the obtained τ_{c1} for

Table 2

Results of Three-Parameter Nonlinear Regression Analysis (single dispersion–eq. 9) of the frequency dependencies of ^{2}H NMR longitudinal relaxation rates for certain protein solutions

Protein	Fitting parameters			SSR [a]
	A (s^{-1})	B ($\times 10^9$)	τ_c (ns)	
Lysozyme, 22°C	4.62 ± 0.33	0.46 ± 0.03	28.6 ± 1.8	3.39
Lysozyme, 4°C	10.15 ± 0.66	0.47 ± 0.03	79.4 ± 4.7	26.46
Alk. phosphatase, 5°C	6.22 ± 0.19	0.08 ± 0.01	108.8 ± 6.3	1.08
10% (w/w) BSA, 18°C	6.50 ± 0.59	0.17 ± 0.02	107.8 ± 9.9	30.80
25% (w/w) BSA, 18°C	13.48 ± 2.40	0.31 ± 0.04	216.2 ± 25.4	602.36
33% (w/w) BSA, 18°C	18.33 ± 1.73	0.36 ± 0.02	310.9 ± 17.5	885.55
Hemocyanin, 25°C	4.54 ± 0.34	0.036 ± 0.007	867.8 ± 29.5	38.75

[a] Sum of squares of the residuals, sum $[(R_{1,meas} - R_{1,calc})^2]$; $R_{1,calc}$ obtained from eqs. (9), (10) and the fitting parameters of this table.

Table 3

Results of five-parameter nonlinear regression analysis (two-dispersions–eq. 11) of the frequency dependencies of ^2H NMR longitudinal relaxation rates for certain protein solutions

Protein	Fitting parameters					SSR [a]
	A (s^{-1})	B_1 ($\times 10^9$)	τ_{c1} (ns)	B_2 ($\times 10^9$)	τ_{c2} (ns)	
Lysozyme, 22°C	4.28 ± 0.26	0.50 ± 0.04	20.2 ± 3.7	0.04 ± 0.05	82.9 ± 40.5	1.46
Lysozyme, 4°C	8.02 ± 0.55	0.48 ± 0.08	18.7 ± 5.6	0.30 ± 0.05	103.4 ± 9.4	6.33
Alk. phosphatase, 5°C	5.93 ± 0.14	0.09 ± 0.01	82.7 ± 8.0	0.004 ± 0.002	472.4 ± 162.2	0.28
10% (w/w) BSA, 18°C	4.97 ± 0.61	0.26 ± 0.04	40.3 ± 11.4	0.04 ± 0.02	227.7 ± 57.8	12.87
25% (w/w) BSA, 18°C [b]	11.76 ± 1.04	0.37 ± 0.02	161.2 ± 10.3	0.003 ± 0.001	4,605.4 ± 1,144.4	85.11
33% (w/w) BSA, 18°C	10.88 ± 2.24	0.50 ± 0.10	63.7 ± 19.2	0.20 ± 0.03	438.6 ± 43.8	373.53
Hemocyanin, 25°C	3.55 ± 0.46	0.03 ± 0.01	187.9 ± 84.9	0.024 ± 0.004	1,072 ± 93.3	23.59

[a] Sum of squares of the residuals, sum $[(R_{1,meas} - R_{1,calc})^2]$.
[b] The measured R_1 values below 10 KHz have been replaced by their average.

10% BSA (Table 3) and 33% BSA (Table 4) are in very good agreement; a slightly longer τ_{rot} is expected for the more concentrated BSA solution as a result of increased intermolecular protein–protein interactions (eq. 4 in ref. [6]).

Although three different τ_{rot} are required to describe the rotation of a nonspherical protein, it is unlikely that these three molecular rotations may be resolved experimentally [39]. The calculated τ_{c2} may not be related with the second

Table 4

Results of seven-parameter nonlinear regression analysis (three dispersions–eq. 12) of the frequency dependencies of ^2H-NMR longitudinal relaxation rates for BSA solutions

Protein	Fitting parameter [a]	SSR [b]
25% BSA, 18°C [c]	$A = 8.31 \pm 1.65\ s^{-1}$,	
	$B_1 = 0.45 \pm 0.29$,	52.12
	$\tau_{c1} = 17.7 \pm 14.0$ ns,	
	$B_2 = 0.31 \pm 0.04$,	
	$\tau_{c2} = 184.7 \pm 17.9$ ns,	
	$B_3 = 0.003 \pm 0.001$,	
	$\tau_{c3} = 4{,}929.4 \pm 1{,}115.8$ ns	
33% BSA, 18°C	$A = 10.02 \pm 2.25\ s^{-1}$,	
	$B_1 = 0.52 \pm 0.13$,	281.50
	$\tau_{c1} = 47.7 \pm 15.9$ ns,	
	$B_2 = 0.25 \pm 0.04$,	
	$\tau_{c2} = 360.4 \pm 44.2$ ns,	
	$B_3 = 0.002 \pm 0.002$,	
	$\tau_{c3} = 4{,}407.1 \pm 3{,}238.1$ ns	

[a] B values must be multiplied by 10^9.
[b] Sum of squares of the residuals, sum $[(R_{1,meas} - R_{1,calc})^2]$.
[c] The measured R_1 values below 10 KHz have been replaced by their average.

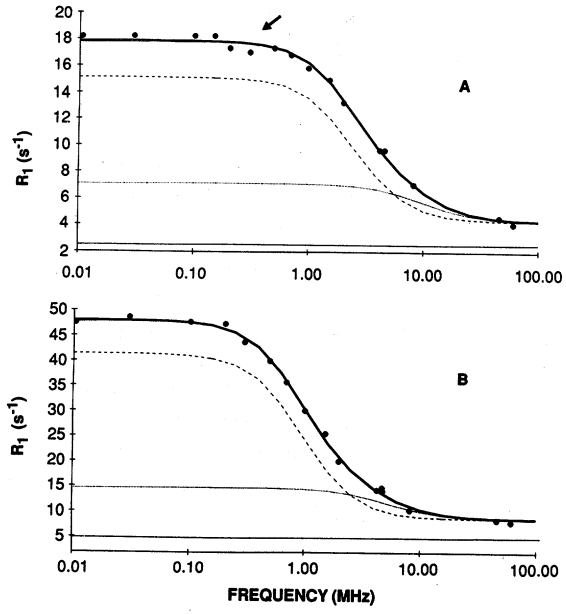

Fig. 1. The field dispersions of ^2H-NMR longitudinal relaxation for hen egg-white lysozyme solutions (210 mg/ml, pH 4.6) at 22°C (A) and 4°C (B); the relaxation rates were measured in a solvent mixture of 80% ^2H_2O/20% ^1H_2O. The solid double curves result from least-squares fittings to the data points (from Figs. 2, 3 of Ref. [13] plus new data at 46.07 and 61.37 MHz) according to eq. (11). The fitting parameters are given in Table 3. In every case, the dotted and broken curves represent the separate contributions $A + Bf(\omega, \tau_{ci})$ of each single dispersion of eq. (11) that correspond to 20.2 and 82.9 ns (22°C) or 18.7 and 103.4 ns (4°C), respectively. The solid straight lines correspond to the ^2H-NMR relaxation rates for the protein-free solvent. The arrow in (A) points at a curve feature that may be due to slowly tumbling protein aggregate(s) with a τ_c of ca. 520 ns which, however, is statistically insignificant.

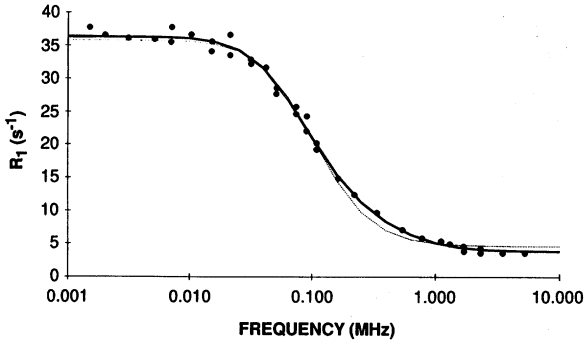

Fig. 2. The field dispersion of ^{2}H-NMR longitudinal relaxation for a *Helix pomatia* α-hemocyanin solution (30:6 mg/ml) in 0.1 *M* phosphate buffer (pH 7.0) made in a solvent mixture of 80% ^2H_2O/20% ^1H_2O at 25°C. Data were obtained from Fig. 3 of Ref. [13]. The solid double curve represents the four-parameter fitting according to eq. (11) with parameters from Table 3; the dotted curve is the three-parameter fitting (eq. 9) with parameters from Table 2.

rotational correlation time of ellipsoid protein molecules: τ_1/τ_2 (Table 6) is significantly closer to unity than τ_{c1}/τ_{c2} (Tables 3, 4) in all cases. The mere fact that dispersion data for the spherical alkaline phosphatase still requires two correlation times suggests that τ_{c2} is unrelated to the (anisotropic) rotation of protein monomers.

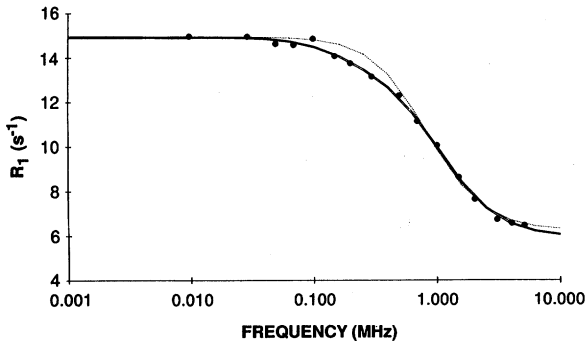

Fig. 3. The field dispersion of ^{2}H-NMR longitudinal relaxation for an *E. coli* alkaline phosphatase (0.3 m*M*) solution in 0.25 *M* Tris, pH/pD 7.5–8.0 at 5°C. Data were obtained from Fig. 6 of Ref. [9]; the ^{2}H-NMR R_1 values of phosphatase samples with solvent D_2O fractions of 0.93, 0.80 and 0.50, were averaged prior to data reduction. The five-parameter fitting (eq. 11, Table 3–solid double curve) is better (0.1% level) than the three-parameter fitting (eq. 9, Table 2–dotted curve).

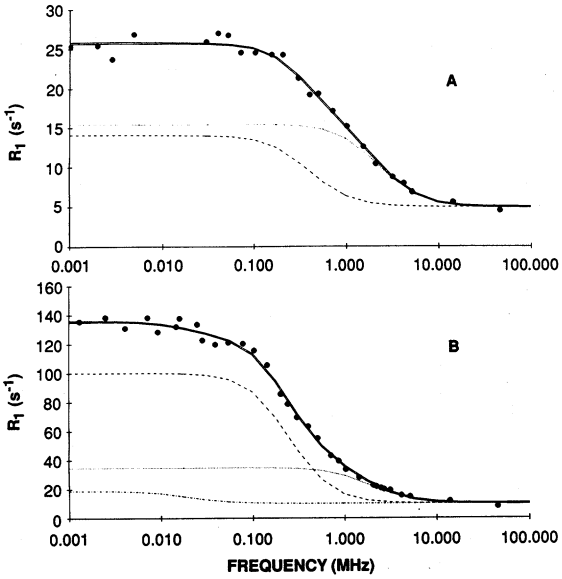

Fig. 4. The field dispersion of ^{2}H-NMR longitudinal relaxation for 10% (A) and 33% (B) w/w BSA solutions in D_2O at 18°C. The solid double curves are the (A) five- or (B) seven-parameter fittings to the data points (Fig. 2 of Ref. [15]); the fitting parameters are given in Tables 3 (10% BSA) and 4 (33% BSA). The broken/dotted curves represent the individual relaxation contributions (eqs. 11 or 12).

The high protein concentrations that are required in dispersion studies of NMR relaxation combined with the occasional absence of salt (which suppresses electrostatic protein–protein interactions) can lead to protein aggregation [6,11] even under experimental conditions that favor the protein monomeric form. Such appears to be the case for lysozyme τ_{c2} which may be identified with τ_{rot} of lysozyme aggregates. This is consistent with the increase in the relative contribution to the dispersion of the slower τ_c with decreasing temperature for lysozyme (B_2 vs. B_1 in Table 3) and with increasing protein concentration for BSA (B_2 vs. B_1 in Tables 3 and 4 for 10% and 33% protein, respectively).

The correlation times τ_{c1} and τ_{c2} for hemocyanin (Table 3) are significantly shorter than τ_{rot} (Table 5). The presence of a small fraction of half size (4.5 10^6 Da) hemocyanin molecules [30] in the sample whose τ_{rot} may account for τ_{c2} cannot explain τ_{c1}. Based on the different timescales of the dynamic processes under consideration (see

Table 5

Calculated and measured protein rotational correlation times

Protein	τ_{rot} (ns)	
	Calculated [a]	Measured [b]
Lysozyme (monomer)	5.5 (22°C), 9.6 (4°C)	10 [c], 7.4 or 4.7 [d]
Alk. phosphatase (dimer)	76.2 (5°C)	Not available
BSA (monomer)	63.0 (18°C)	41 [e], 62 [f]
Hemocyanin	7,386.7 (25°C)	Not available

[a] In the case of ellipsoids (Table 1) considering a sphere of radius $r_s = R_G + 3$ Å, R_G being the protein radius of gyration, from $\tau_{rot} = 4\pi n r_s^3/(3kT)$ where $k = 1.38 \times 10^{-16}$ erg.k^{-1}. The R_G values used are 13.8 Å (lysozyme–Refs. [12,25], 33 Å (BSA–Refs. [12,19], and 184 Å (hemocyanin, Ref. [41]); for alkaline phosphatase, $r_s = 33$ Å (Table 1). The viscosity of the various solvents at different temperatures were obtained by linear intrapolation from data in the CRC Handbook of Chemistry and Physics 67th edn. (ed. R.C. Weast). The isotopic composition of the solvent was taken into account, assuming that, as at 25°C, ^2H_2O is 23% more viscous than ^1H_2O. The solvent n values (in CP) used in the calculation of τ_{rot} were: 1.855 and 1.130 (lysozyme at 4 and 22°C, respectively, 1.944 (alkaline phosphatase), 1.295 (BSA), and 1.109 (hemocyanin).

[b] Reported values can be directly compared to τ_{rot} obtained from NMR: they are one-third of the corresponding Debye correlation times obtained from dielectric relaxation or light scattering [16,20,21,39].

[c] From light scattering, according to $\tau_{rot} = (6D_{rot})^{-1}$, for 15% protein at 20°C [40].

[d] From ^{17}O-NMR: 7.4 ns for 8% protein at 27°C (in the absence of salt) and 4.7 ns for 10% protein in 0.1 M NaCl at 21°C [11].

[e] From dielectric relaxation, as $\tau/3$ (see above) for 1% protein at 23°C [43].

[f] From dielectric relaxation, as the one-third of the harmonic mean of $\tau_{\epsilon 1}$ and $\tau_{\epsilon 2}$, for ca. 10% protein at 25°C [42].

Introduction) one may identify τ_{c1} for hemocyanin with τ_{lat}. The hemocyanin τ_{rot} is sufficiently slow so that the contribution of lateral diffusion to τ_{Bs} may become dominant (eq. [6]). The longest (μs range) correlation times for 25% or 33% BSA (Table 4) are peculiar to these samples and should be attributed to protein aggregation.

4.3 Estimates of hydration

An inspection of eqs. (2)–(5) and (10)–(12) can relate the fitting parameters B_i ($i = 1, 2, \ldots$) with the amount of 'bound' water. Specifically, if we assume an isotropic or an anisotropic model

$$\sum_i B_i = \frac{3\pi^2}{10} \frac{2I+3}{I^2(2I-1)} K^2 \left(1 + \frac{\eta^2}{3}\right) P_B \qquad (14)$$

or

$$\sum_i B_i = \frac{3\pi^2}{10} \frac{2I+3}{I^2(2I-1)} K^2 S^2 P_B \qquad (15)$$

where P_B is the number-average fraction of 'bound' water for the coexisting protein species. From eqs. (14) and (15), P_B can be estimated and the amount n_H of 'bound' water (g ^2H_2O/100 g protein in a system containing C g protein/ml or W g protein/100 g will be given by:

$$n_H = P_B \frac{(1 - C\bar{V})\rho}{C} 100 \qquad (16)$$

or

$$n_H = P_B \frac{100 - W}{W} 100 \qquad (17)$$

where $\bar{V}$ is the protein's specific volume and ρ the density of ^2H_2O (~ 1.1 g/ml); a correction factor for the solvent's isotopic composition may be required (1.25 for 80% ^2H_2O–20% ^1H_2O). The so calculated amounts of 'bound' water for different S-values are given in Table 7. The results may underestimate (monomer) hydration

Table 6

Calculated rotational correlation times of proteins modelled as prolate ellipsoids of revolution [a]

Protein	Correlation times (ns)		
	τ_0 [b]	τ_1	τ_2
Lysozyme	9.6 (22°C)	11.0	9.6
	16.7 (4°C)	19.2	16.7
BSA	54.8 (18°C)	134.9	62.6

[a] According to Perrin as corrected by Koenig [44], for rotation about the long (τ_2) or the short (τ_1) axis. The molecular dimensions of Table 1 were increased by a 3-Å solvent layer.

[b] The isotropic correlation time τ_0 for a sphere of equal volume to an ellipsoid of long axis $2a$ and short axis $2b$, is given by $\tau_0 = 4\pi n a b^2/(3kT)$; the viscosity values n used are those of Table 5.

(19,20,28,39,41] when some protein is in the form of aggregates. As expected, hydration decreases with increasing temperature (lysozyme), and increasing protein concentration (BSA) when protein–water interactions are being replaced with protein–protein interactions.

Recent studies of protein hydration in solution by multi-dimensional NMR techniques [47,48] have identified water molecules buried in the protein interior that stabilize the protein conformation through hydrogen-bond bridges and which constitute an integral part of the protein structure [1]. Their number (of the order of 10 molecules/molecule of medium-sized protein) is but a small fraction of general protein hydration estimates (typically 33 g 'bound' water/100 g of protein or 300 molecules/molecule of medium sized protein—ref. [39]). Interestingly, it agrees well with hydration estimates from field dispersion data (Table 7) for $S = 1$, i.e. for isotropic motion of 'bound' water. It is likely that the observed NMR field dispersion of protein solutions is due to this irrotationally 'bound' water that tumbles isotopically with the protein molecules. Other hydration water molecules at the disordered and dynamic protein surface must have correlations times shorter than 1 ns [47,48], comparable to the correlation times (10–100 ps) of mobile protein side chains [49,50] whose field dispersion is beyond the experimentally accessible NMR frequency range.

5. Conclusions

In the past, field dispersion data for protein solutions have been fitted well by the Cole–Cole equation [9,14] which being simply heuristic, has no *a priori* validity. The so obtained correlation times $\tau_c = (2n\nu_c)^{-1}$ (159 ns or 61 ns for lysozyme at 4 or 22°C, respectively, 175 ns for alkaline phosphatase and 1,616 ns for hemocyanin—refs. [9,13,14]) are approximately twice as long as our single dispersion results (Table 2) which, with the exception of hemocyanin, already exceed our best estimates of τ_{rot} (Table 1).

Recently, Schauer et al. [15] modelled the ^{2}H-NMR T_1 dispersion of, among others, protein solutions using a single dispersion. They found a correlation time of 2.7 10^{-7} s for BSA at 18°C (comparable to our single dispersion results—Table 2) which they identified with τ_{rot} without explaining the difference from the known $\tau_{rot} \sim 40$ ns of BSA monomers [39]. In their fittings (Fig. 2 of ref. [15]), T_1's for protein solutions are systematically overestimated below the inflection frequency and underestimated above it, as in Figs. 2 and 3 (single dispersions) of the present study.

The need for an additional contribution to NMR relaxation in order to fit the deuterium T_1 field dependence data for protein solutions has been previously identified [10]; the second relaxation component was attributed to deuterium chamical exchange between ^2H_2O and protein

Table 7

Estimates of protein hydration from the ^{2}H NMR T_1 field dispersion data

Protein	Protein concentration	Hydration [a] (g ^2H_2O/100 g protein)		
		$S = 1.00$ [b]	$S = 0.12$ [b]	$S = 0.23$ [b]
Lysozyme, 22°C	210 mg/ml	0.4	30.2	8.2
Lysozyme, 4°C	210 mg/ml	0.6	43.6	11.9
Alk. phosphatase, 5°C	0.3 mM, 25.5 mg/ml	0.7	39.8	10.0
10% BSA, 18°C	10 mg/90 mg ^2H_2O	0.4	27.1	7.4
33% BSA, 18°C	33 mg/67 mg ^2H_2O	0.2	15.6	4.7
Hemocyanin, 25°C	30.6 mg/ml	0.3	23.7	6.5

[a] Calculated from the B_i values of the best fittings according to eqs. (14)–(17). The specific volume of lysozyme is 0.70 ml/g; that of the other proteins 0.73 ml/g.

[b] Order parameter for the isotropic ($S = 1$) or anisotropic ($S < 1$) motion of water molecules 'bound' to the protein.

ionizable groups on the basis of the observed difference(s) between the ^2H and ^{17}O-NMR normalized (mostly transverse) relaxation rates [10, 11]. Recently, the occurrence of proton chemical exchange in protein solutions has been demonstrated by ^1H-NMR transverse relaxation measurements [36]. Transverse relaxation is sensitive to slow motions such as hydrogen chemical exchange (timescale of 10^{-4} s—see Section 1) at all NMR frequencies as a result of its zero-frequency spectral density term. Longitudinal relaxation on the other hand is brought about by motions near the Larmor frequency (or its double) and should be little affected by slow processes (such as chemical exchange) at NMR frequencies well above 10 KHz. Indeed, there is no evidence of ms motions for any sample (Tables 2–5) and the lack of data around 1 KHz makes deuterium chemical exchange an unlikely contributor to the deuterium T_1 field dispersion of protein solutions in the frequency range 0.1–10 MHz.

Estimates of τ_{lat} from the measured translational diffusion D_{lat} of water molecules near a protein (BSA) surface [37] yield $\tau_{lat} = \tau^2/6\ D_{lat} \sim 6$ ns, a considerably shorter value than τ_{c1} obtained from the analysis of the ^2H-NMR T_1 field dispersion data for hemocyanin. However, this value (6 ns) refers to an average distance of 10 Å from the protein surface and is most likely intermediate between that of free water and the τ_{lat} in the immediate vicinity of the protein surface.

It may be argued that the analysis of biological NMR relaxation data in terms of continuous distributions of correlation times rather than discrete components, is a more realistic approach [5,45]. However, in the absence of experimental evidence about the form and the extent of such distributions, adjustable parameters must be introduced. This by itself can result in good fitting of the data regardless of whether the assumed distribution is proper or not.

References

1 H.J.C. Berendsen, Specific interactions of water with biopolymers, ed. F. Franks, in: Water—A comprehensive treatise, vol. 5. (Plenum Press, New York, NY, 1975) pp. 293–349.

2 K.J. Packer, The dynamics of water in heterogeneous systems, Phil. Trans. R. Soc. London B 278 (1977) 59–87.

3 R.G. Bryant, NMR relaxation studies of solute–solvent interactions, Annu. Rev. Phys. Chem. 29 (1978) 167–188.

4 W. Derbyshire, The dynamics of water in heterogeneous systems with emphasis on subzero temperatures, ed. F. Franks in: Water—A comprehensive treatise, vol. 7 (Plenum Press, New York, NY, 1982) pp. 339–469.

5 L.J. Lynch, Water relaxation in heterogeneous and biological systems, in: ed. J.S. Cohen, Magnetic resonance in biology, vol. 2 (Wiley, New York, NY, 1984) pp. 248–304.

6 H. Pessen and T.F. Kumosinski, Measurements of protein hydration by various techniques, in: eds. C.H.W. Hirs and S.N. Timasheff, Methods in enzymology, vol. 117 (Academic Press, Orlando, FL, 1985) pp. 219–255.

7 R.G. Bryant and B. Halle, NMR relaxation of water in heterogeneous systems—Consensus views?, in: ed. F. Franks, Biophysics of water—Proceedings of a working conference (Wiley Interscience, New York, NY, 1982) pp. 389–393.

8 H.T. Edzes and E.T. Samulski, The measurement of cross-relaxation effects in the proton NMR spin–lattice relaxation of water in biological systems: Hydrated collagen and muscle, J. Magn. Reson. 31 (1978) 207–229.

9 S.H. Koenig, R.G. Bryant, K. Hallenga and G.S. Jacob, Magnetic cross-relaxation among protons in protein solutions, Biochemistry 17 (1978) 4348–4358.

10 L. Piculell and B. Halle, Water spin relaxation in colloidal systems. Part 2—^{17}O and ^2H relaxation in protein solutions, J. Chem. Soc. Faraday Trans. I, 82 (1986) 401–414.

11 L.T. Kakalis and I.C. Baianu, Oxygen-17 and deuterium nuclear magnetic relaxation studies of lysozyme hydration in solution: Field dispersion, concentration, pH/pD, and protein activity dependencies, Arch. Biochem. Biophys. 267 (1988) 829–841.

12 B. Halle, T. Anderson, S. Forsén and B. Lindman, Protein hydration from water oxygen-17 magnetic relaxation, J. Am. Chem. Soc. 103 (1981) 500–508.

13 S.H. Koenig, K. Hallenga and M. Shporer, Protein–water interactions studied by solvent ^1H, ^2H, and ^{17}O magnetic relaxation, Proc. Natl. Acad. Sci. USA 72 (1975) 2667–2671.

14 K. Hallenga and S.H. Koenig, Protein rotational relaxation as studied by solvent ^1H and ^2H magnetic relaxation, Biochemistry 15 (1976) 4255–4264.

15 G. Schauer, R. Kimmich and W. Nusser, Deuteron field-cycling relaxation spectroscopy and translational water diffusion in protein hydration shells, Biophys. J. 53 (1988) 397–404.

16 A. Abragam, Principles of nuclear magnetism (Oxford University Press, New York, NY, 1961) pp. 264–353.

17 P. Waldstein, S.W. Rabideau, and J.A. Jackson, Nuclear magnetic resonance of single crystals of D_2O ice, J. Chem. Phys. 41 (1964) 3407–3411.

18 B. Halle and L. Piculell, Water spin relaxation in colloidal

systems. Part 3—Interpretation of the low-frequency dispersion, J. Chem. Soc. Faraday Trans. I, 82 (1986) 415–429.
19 C. Tanford, Physical chemistry of macromolecules (Wiley, New York, NY, 1961) pp. 307, 317–456.
20 C.R. Cantor and P.R. Schimmel, Biophysical chemistry, Part II (W.H. Freeman and Co., San Francisco, CA, 1980) pp. 539–590.
21 C.P. Poole, Jr. and H.A. Farach, Relaxation in magnetic resonance (Academic Press, New York, NY, 1971) pp. 62–89, 221–240.
22 M.R. Bruzzesi, E. Chiancone and E. Antonini, Association–dissociation properties of lysozyme, Biochemistry, 4 (1965) 1796–1800.
23 O.G. Hampe, Conformation of lysozyme in aqueous solution, Eur. J. Biochem. 31 (1972) 32–37.
24 S.K. Banerjee, A. Pogolotti and J.A. Rupley, Self-association of lysozyme, J. Biol. Chem. 250 (1975) 8260–8266.
25 T. Imoto, L.N. Johnson, A.C.T. North, D.C. Phillips and J.A. Rupley, Vertebrate lysozymes, in: ed. P.D. Boyer The enzymes, vol. VII. (Academic Press, New York, NY, 1972) pp. 665–868.
26 T.W. Reid and I.B. Wilson, *E. coli* alkaline phosphatase, in: ed. P.D. Boyer, The enzymes, vol. IV (Academic Press, New York, NY, 1971) pp. 373–415.
27 M.L. Applebury and J.E. Coleman, *Escherichia coli* alkaline phosphatase, J. Biol. Chem. 244 (1969) 308–318.
28 T. Peters, Jr., Serum albumin, Adv. Prot. Chem. 37 (1985) 161–245.
29 J.E. Mellema and A. Klug, Quaternary structure of gastropod hemocyanin, Nature 239 (1972) 146–150.
30 R.J. Siezen and R. van Driel, Structure and properties of hemocyanins, XIII, J. Mol. Biol. 90 (1974) 91–102.
31 R.J. Siezen and E.F.J. van Bruggen, Structure and properties of hemocyanins, XII, J. Mol. Biol. 90 (1974) 77–89.
32 K.E. van Holde and K.I. Miller, Hemocyanins, Quart. Rev. Biophys. 15 (1982) 1–129.
33 J.R. Knox and H.W. Wyckoff, A crystallographic study of alkaline phosphatase at 7.7 Å resolution, J. Mol. Biol. 74 (1973) 533–545.
34 R.I. Jennrich and M.L. Ralston, Fitting nonlinear models to data, Annu. Rev. Biophys. Bioeng. 8 (1979) 195–238.
35 W.H. Beyer, CRC Standard mathematical tables (CRC Press, Boca Raton, FL, 1984).
36 B.P. Hills, S.F. Takacs and P.S. Belton, The effects of proteins on the proton NMR transverse relaxation times of water, Mol. Phys. 67 (1989) 903–918.
37 C.F. Polnaszek and R.G. Bryant, Nitroxide radical induced solvent proton relaxation: Measurement of localized translation diffusion, J. Chem. Phys. 81 (1984) 4038–4045.
38 A.C. McLaughlin and J.S. Leigh, Jr., Relaxation times in systems with chemical exchange: Approximate solutions for the nondilute case, J. Magn. Res. 9 (1973) 296–304.
39 I.D. Kuntz, Jr. and W. Kauzmann, Hydration of proteins and polypeptides, Adv. Protein Chem. 28 (1974) 239–345.
40 S.B. Dubin, N.A. Clark and G.B. Benedek, Measurement of the rotational diffusion coefficient of lysozyme by depolarized light scattering: Configuration of lysozyme in solution, J. Chem. Phys. 54 (1971) 5158–5164.
41 J. Berger, I. Pilz, R. Witters and R. Lontie, Studies by small-angle X-ray scattering of the quaternary structure of the α-hemocyanin of *Helix pomatia*, Eur. J. Biochem. 80 (1977) 79–82.
42 P. Moser, P.G. Squire and C.T. O'Konski, Electric polarization in proteins—Dielectric dispersion and Kerr effect studies of isoionic bovine serum albumin, J. Phys. Chem. 70 (1966) 744–756.
43 P. Ingram and H.G. Jerrard, Measurement of relaxation times of macromolecules by the Kerr effect, Nature 196 (1962) 57–58.
44 F. Perrin, Mouvement Brownien d'un ellipsoide (I). Dispersion dielectrique pour des molecules ellipsoidales, J. Phys. Radium VII 5 (1934) 497–511; S.H. Koenig, Brownian motion of an ellipsoid. A correction to Perrin's results, Biopolymers 14 (1975) 2421–2423.
45 R.M. Kroeker and R.M. Henkelman, Analysis of biological NMR relaxation data with continuous distributions of relaxation times, J. Magn. Res. 69 (1986) 218–235.
46 B. Halle and H. Wennerström, Interpretation of magnetic resonance data from water nuclei in heterogeneous systems, J. Chem. Phys. 75 (1981) 1928–1943.
47 G. Otting and K. Wüthrich, Studies of protein hydration in aqueous solution by direct NMR observation of individual protein-bound water molecules, J. Am. Chem. Soc. 111 (1989) 1871–1875.
48 G.M. Clore, A. Bax, P.T. Wingfield and A.M. Gronenborn, Identification and localization of bound internal water in the solution structure of interleukin 1β by heteronuclear three-dimensional ^{1}H rotating-frame Overhauser ^{15}N–^{1}H multiple quantum coherence NMR spectroscopy, Biochemistry 29 (1990) 5671–5676.
49 G. Wagner and K. Wüthrich, Observation of internal mobility of proteins by nuclear magnetic resonance in solution, in: eds. C.H.W. Hirs and S.N. Timasheff, Methods in enzymology, vol. 131 (Academic Press, Orlando, FL, 1986) pp. 307–326.
50 R.E. London, Interpreting protein dynamics with nuclear magnetic resonance relaxation measurements, in: eds. N.J. Oppenheimer and T.L. James, Methods in enzymology, vol. 176 (Academic Press, San Diego, CA, 1989) pp. 358–375.